The GSTAR (1;1) Modelling with Three Combination of the Grid Sizes and Spatial Weight Matrix in Forest Fires Cases

Muhammad Yahya Ayyash[1], Nur'ainul Miftahul Huda[2], Nurfitri Imro'ah[1]
[1]Statistics Departement, Universitas Tanjungpura, Indonesia
[2]Mathematics Departement, Universitas Tanjungpura, Indonesia
nurainul@fmipa.untan.ac.id

ABSTRACT

One of the models that is utilized in spatio-temporal analysis is known as the Generalized Space-Time Autoregressive (GSTAR). This model incorporates two dimensions, namely the geographical and temporal aspects of the situation. This approach assists in the identification of patterns and correlations between data by taking into account both spatial and temporal elements. From modeling the confidence level of forest fire hotspot cases in Kubu Raya and its surrounds using the GSTAR (1;1) model with three different combinations of grids and special weight matrices, the purpose of this study is to discover which combination of grids and spatial weight matrices is the most effective. The results of diagnostic tests and the degrees of MAPE accuracy are used to determine which model is the most suitable. The data was obtained from the FIRMS-NASA platform, ranging from January 2014 to August 2024. A grid with a dimension of 1.25 x 1.25 degrees and a rook contiguity weight matrix is a combination of grids and spatial weight matrices that meet the white noise assumption, according to the findings of the study. This conclusion is based on the diagnostic test. As a result, the combination of a grid with a size of 1.25 x 1.25 and a rook contiguity weight matrix is the best in this modeling. This combination has a MAPE of 11.797%, which indicates that this model has a good level of accuracy.

———————————— ◆ ————————————

A. INTRODUCTION

Analysis of spatial and temporal relationships is a significant strategy for understanding of phenomena that are simultaneously influenced by location and time (Lu et al., 2021). Researchers are able to recognize patterns, correlations, and distributions of variables in two dimensions, namely location and time, through the utilization of this methodology. Comparatively, temporal analysis focuses on changes or dynamics that take location across time (Zhao et al., 2021). In contrast, spatial analysis investigates the geographic influence that exists between objects or phenomena that are dispersed across several different locations (Franch-Pardo et al., 2020). Due to the fact that it takes into consideration the complexity of spatial and temporal fluctuations, the combination of the two provides a more in-depth understanding of the phenomenon that is being investigated. The Generalized Space-Time Autoregressive (GSTAR) model is frequently utilized in the process of spatial-temporal analysis (Hestuningtias & Kurniawan, 2023). GSTAR has been used for discrete data in previous research, which broadens the scope of this model's application in analysing a wider variety of spatial-temporal data (Huda et al., 2021). In a different investigation, GSTAR was utilized to find

outliers, exemplifying the model's capacity to recognize anomalies or departures from the overall trend in the examined data (Huda et al., 2022). However, the GSTAR(1;1) model has also been utilized in a dengue case study, which demonstrates the model's applicability in simulating the spatial-temporal spread of the disease and highlights the potential application of the model in public health studies (Mukhaiyar et al., 2019).

The GSTAR model explains the manner in which patterns of change and interactions between locations within a spatial-temporal system. The determination of the weighting matrix, which is frequently a matter of opinion, is one of the difficulties that arise while utilizing the GSTAR model (Zhu et al., 2022). The selection of this weighting matrix has a significant impact on the findings of the research by virtue of the fact that it is utilized to ascertain the degree to which a certain location exerts an influence on other locations depending on specific criteria (Lam & Souza, 2019). Previous studies used kernel functions to apply a new weight matrix, which provided an original technique for comprehending the spatial linkages present in the GSTAR model (Yundari et al., 2018). Modifications to the weight matrix have been done to enhance the accuracy of the GSTAR(1;1) algorithm, which has proven to be an essential step in enhancing the performance of the model (Pasaribu et al., 2021). The GSTAR(1;1) model has been the subject of recent research focusing on analyzing different weight matrices and comparing their success in describing interdependence between locations in spatial-temporal information (Huda & Imro'ah, 2023).

The purpose of the weight matrix in the GSTAR model is to serve as a representation of the strength of the association between locations based on spatial criteria. These factors include geographic distance and regional features (Huda et al., 2023). When selecting the incorrect weight matrix, it is possible to generate inaccurate estimates and to have an impact on the validity of the analysis results. The purpose of this research is to evaluate and contrast a number of different types of weight matrices, including uniform, queen contiguity, and rook contiguity. Determining the grid is yet another obstacle that must be overcome in the GSTAR concept. In the context of the study area, grids are geographical units that represent specific locations (Ryerson et al., 2022). The selection of the appropriate grid size significantly impacts the level of precision and accuracy of the analysis results. The grid is a spatial unit that represents specific locations within the study region (Ramsdale et al., 2017). In order to determine which grid size is most effective in displaying spatial-temporal data, this study examines and evaluates numerous grid sizes, including 0.50 × 0.50 degrees, 1.00 × 1.00 degrees, and 1.25 × 1.25 degrees. Forest fires are an example of a phenomenon that combines spatial and temporal analysis. This event involves complicated spatial and temporal fluctuations, one example of a phenomenon combining these two types of analysis.

Forest fires are a phenomenon that is highly dependent on spatial-temporal variables (Dastour et al., 2024). The patterns of fire spread are controlled by geographic elements such as the kind of land and the altitude and by temporal factors such as the changing of the seasons and the weather (Wu et al., 2022). Forest fires have become a persistent and widespread concern in Indonesia, particularly in regions containing agricultural peatlands. There is a high incidence of forest fires in Indonesia, frequently caused by human activities and made worse by favorable environmental conditions, such as extended dry seasons. West Kalimantan is a region that is regularly vulnerable to forest fires. This province is highly susceptible to fires

because most of its land comprises peatland, and the equator crosses its geographical position. Peatlands are characterized by the fact that they are easily combustible and can store significant quantities of biomass, litter, and mineral soil on their surface (Rachman et al., 2020). The Kubu Raya Regency is one of the regions in West Kalimantan that is prone to forest fires during the dry season. This region is one of the areas that frequently see forest fires (Arifa, 2022). In this context, spatial-temporal analysis through the GSTAR model can provide a better knowledge of fire patterns, enable forecasts of sensitive areas, and assist in making decisions that are more informed in forest fire mitigation and control activities. This research aims to establish which grid size is the most effective by contrasting three different grid sizes: 0.50 × 0.50, 1.00 × 1.00, and 1.25 × 1.25. It will also examine the utilization of three distinct kinds of spatial weight matrices, namely uniform, queen contiguity, and rook contiguity, and compare and contrast their respective applications.

B. METHODS
1. Generalized Space Time Autoregressive (GSTAR) (1;1) Model

The GSTAR (1;1) model is an example of a generalized space-time autoregressive model type. First-order spatial lag and temporal lag are also incorporated into this approach. Within geography, "first-order spatial lag" describes a spatial relationship in which observations taken at one location are influenced by observations made at locations close to the location. On the other hand, first-order temporal lag presents evidence of a temporal link within the framework of a temporal structure. This suggests a temporal relationship between the period in question and the present observations, influenced by past observations at the same location. In 2002, Borovkova, Lopuha, and Ruchjana were the individuals who put forward the GSTAR model for the first time. The Autoregressive (AR) and Space-Time Autoregressive (STAR) models were the foundation for the development of the GSTAR model, which is capable of managing time series data that possess heterogeneous spatial features (Ilmi et al., 2023). The discipline of statistical analysis has made a crucial step forward with this development. This is a significant advancement in the field of statistical analysis. It is possible to state the GTAR (1;1) model in the following manner (Ruchjana et al., 2012):

$$Y_t = \Phi_{10} W^{(0)} Y_{t-1} + \Phi_{11} W^{(1)} Y_{t-1} + e_t \tag{1}$$

where Y_t is observations in period t, Y_{t-1} is observations in periode $t-1$, Φ_{10} is autoregressive coefficients for the influence of the location itself, Φ_{11} is autoregressive coefficients for the influence of neighboring locations, $W^{(0)}$ is identity matrix, $W^{(1)}$ is spatial weight matrix, and e_t is error in period t. Alternatively, Equation (1) can be expressed as:

$$\begin{bmatrix} Y_t^{(1)} \\ Y_t^{(2)} \\ \vdots \\ Y_t^{(N)} \end{bmatrix} = \begin{bmatrix} \phi_{10}^{(1)} & 0 & \cdots & 0 \\ 0 & \phi_{10}^{(2)} & \cdots & 0 \\ \vdots & \vdots & \ddots & \vdots \\ 0 & 0 & \cdots & \phi_{10}^{(N)} \end{bmatrix} \begin{bmatrix} Y_{t-1}^{(1)} \\ Y_{t-1}^{(2)} \\ \vdots \\ Y_{t-1}^{(N)} \end{bmatrix} + \begin{bmatrix} \phi_{11}^{(1)} & 0 & \cdots & 0 \\ 0 & \phi_{11}^{(2)} & \cdots & 0 \\ \vdots & \vdots & \ddots & \vdots \\ 0 & 0 & \cdots & \phi_{11}^{(N)} \end{bmatrix} \begin{bmatrix} 0 & w_{12} & \cdots & w_{1N} \\ w_{21} & 0 & \cdots & w_{2N} \\ \vdots & \vdots & \ddots & \vdots \\ w_{N1} & w_{N2} & \cdots & 0 \end{bmatrix} \begin{bmatrix} Y_{t-1}^{(1)} \\ Y_{t-1}^{(2)} \\ \vdots \\ Y_{t-1}^{(N)} \end{bmatrix} + \begin{bmatrix} e_t^{(1)} \\ e_t^{(2)} \\ \vdots \\ e_t^{(N)} \end{bmatrix}$$

2. Spatial Weight Matrix

One of the most important components of the GSTAR model is the spatial weight matrix, which illustrates the connection between one location and another. When it comes to finding the spatial weight value, the conditions that need to be fulfill are as follows: $w_{ii} = 0$ and $\sum_{i \neq j} w_{ij} = 1$; where $i = 1, 2, ..., N$ and $j = 1, 2, ..., N$. From a broad standpoint, the spatial weight matrix can be described as (Huda & Imro'ah, 2023):

$$W = [w_{ij}] = \begin{bmatrix} 0 & w_{12} & ... & w_{1N} \\ w_{21} & 0 & ... & w_{2N} \\ \vdots & \vdots & \ddots & \vdots \\ w_{N1} & w_{N2} & ... & 0 \end{bmatrix}$$

Choosing the appropriate spatial weight matrix is critical in spatial data analysis since it helps one comprehend the connections between different locations. Uniform is all spatial units are assumed to have the same weight across the board (Mukhaiyar et al., 2019). Queen contiguity is two spatial units are regarded to be neighbors if they share an edge or a corner. Rook contiguity is two spatial units are regarded as neighbors if they share the same edge (Suryowati et al., 2023). Those are the three main forms of spatial weight matrices utilized frequently.

3. Grid

Grid is a system that is used to depict an object's position on the earth's surface based on the object's latitude and longitude coordinates (Ware et al., 2020). Longitude is an imaginary line that connects the north and south poles, whereas latitude is an imagined line that circles the earth parallel to the equator. Both of these lines are considered to be hypothetical locations. Determining a particular position on Earth is made possible by utilizing this grid, which is of great significance in various sectors, including mapping, navigation, and spatial data analysis (Bill et al., 2022).

C. RESULT AND DISCUSSION

The data utilized in this investigation was obtained from the FIRMS - NASA (Fire Information for Resource Management System) platform. This platform offers real-time information on forest fires all around the world. The dataset utilized is known as the forest fire confidence level, which corresponds to the degree of certainty that hotspots identified by satellites are indicative of forest fires within the area. Ten years of historical data pertinent to examining forest and land fire patterns are covered by the data period that is employed, which extends from January 2014 to August 2024.

Kubu Raya Regency was chosen as the area of concentration for this research among all the regions that comprise West Kalimantan. There is a compelling rationale for choosing Kubu Raya as a case study. This region is a potential research subject for forest fire investigation due to its distinctive characteristics. One primary reason is that Kubu Raya has a relatively high average number of fires. Figure 1 shown that Kubu Raya Regency is fourth in the number of forest and land fire cases, after Ketapang, Sanggau, and Sintang Regencies. The fact that Kubu Raya is

located in this position demonstrates that it is one of the areas that has a substantial level of fire vulnerability, as shown in Figure 1.
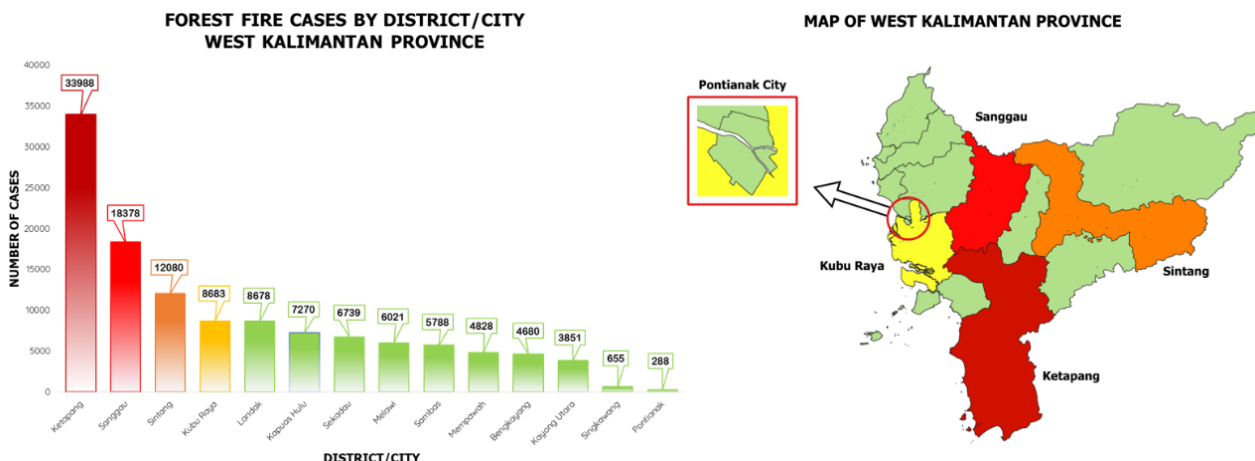

Figure 1. Map and Number of Cases of Forest Fires in West Kalimantan (2014-2023)
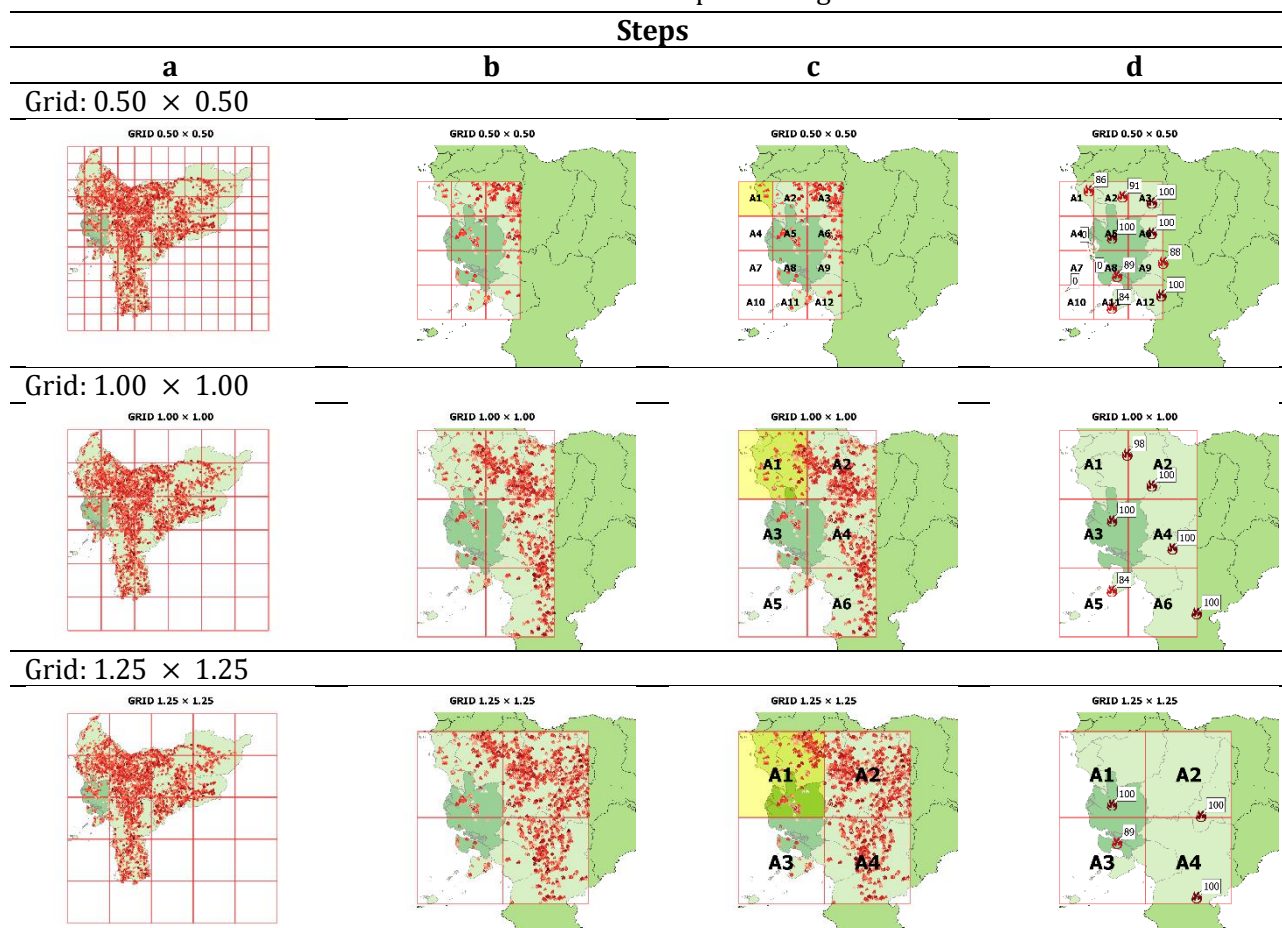
1. Data Preprocessing

In order to divide the study area, the analysis region is first divided into grid cells of a size specified in advance. When studying forest fires, the grid method is utilized as an alternative to the utilization of administrative borders such as districts. The decision to employ grids as an alternative to administrative location units (districts) was taken because the distribution of forest fires within a district can vary dramatically from one district to the next. A grid system can give a more precise representation of the local differences in forest fire occurrences. Before the grid was established, the number of hotspots located in Kubu Raya Regency during the previous ten years was 5,206 points. The number of hotspots for each grid was determined after the grid was formed. The hotspots for each grid were 0.50 × 0.50 degrees, which resulted in 12,446 points; 1.00 × 1.00 degrees, which resulted in 30,319 points; and 1.25 × 1.25 degrees, which resulted in 30,346 points. The followings are the preprocessing data's step.

a. Grid Classification. The initial step in the data preprocessing stage involves the creation of grids with three distinct sizes. These grids span a range of angles, specifically 0.50 × 0.50 degrees (12 locations), 1.00 × 1.00 degrees (6 locations), and 1.25 × 1.25 degrees (4 locations). During the grid generation process, a map of West Kalimantan is utilized. When conducting the spatial-temporal analysis with the GSTAR model, the number of grid cells acquired from each size will provide the location units that will be utilized. The details of grid classification can be seen in Table 1 (first column).

b. Monthly Data Filter. The data on forest fires is organized into monthly intervals according to the size of each grid that has been created. The process of filtering the data is carried out for each month from January 2014 to August 2024. Which can be seen in Table 1 (second column).

c. Monthly Data Filter per Location. This procedure creates data focused on each location that reflects a specific location, depending on grid sizes of 0.50 × 0.50 degrees, 1.00 × 1.00 degrees, and 1.25 × 1.25 degrees. Which can be seen in Table 1 (third column).

d. Maximum Value Selection. The maximum value is selected to provide a description of the forest fire instances that have the highest intensity in each location within a specific time period. Particularly in the context of employing the GSTAR model for spatial-temporal analysis, this value serves as the foundation for the study because it guarantees that the most serious fire cases are considered. Which can be seen in Table 1 (fourth column).

This is the visualization of the data preprocessing is shown in Table 1.

Table 1. Data Preprocessing

Steps			
a	**b**	**c**	**d**
Grid: 0.50 × 0.50			
Grid: 1.00 × 1.00			
Grid: 1.25 × 1.25			

2. Descriptive Statistics

The data obtained for three grid sizes, namely grid 0.50 × 0.50 degrees, grid 1.00 × 1.00 degrees, and grid 1.25 × 1.25 degrees, were obtained after the data preprocessing. These grid sizes were based on the data obtained from forest fire hotspots. The number of observations collected is 127, and the period covered by these observations is from January 2014 to August 2024. The data represents each location, which reflects hotspots in detecting forest fires. A visual representation of the hotspot data plot for forest fire cases is presented in Figure 2. The following is a descriptive analysis that provides a numerical summary to help better understand the data's characteristics. These descriptive statistics play an important part in obtaining a through image of the data distribution during the research period shown in Table 2.
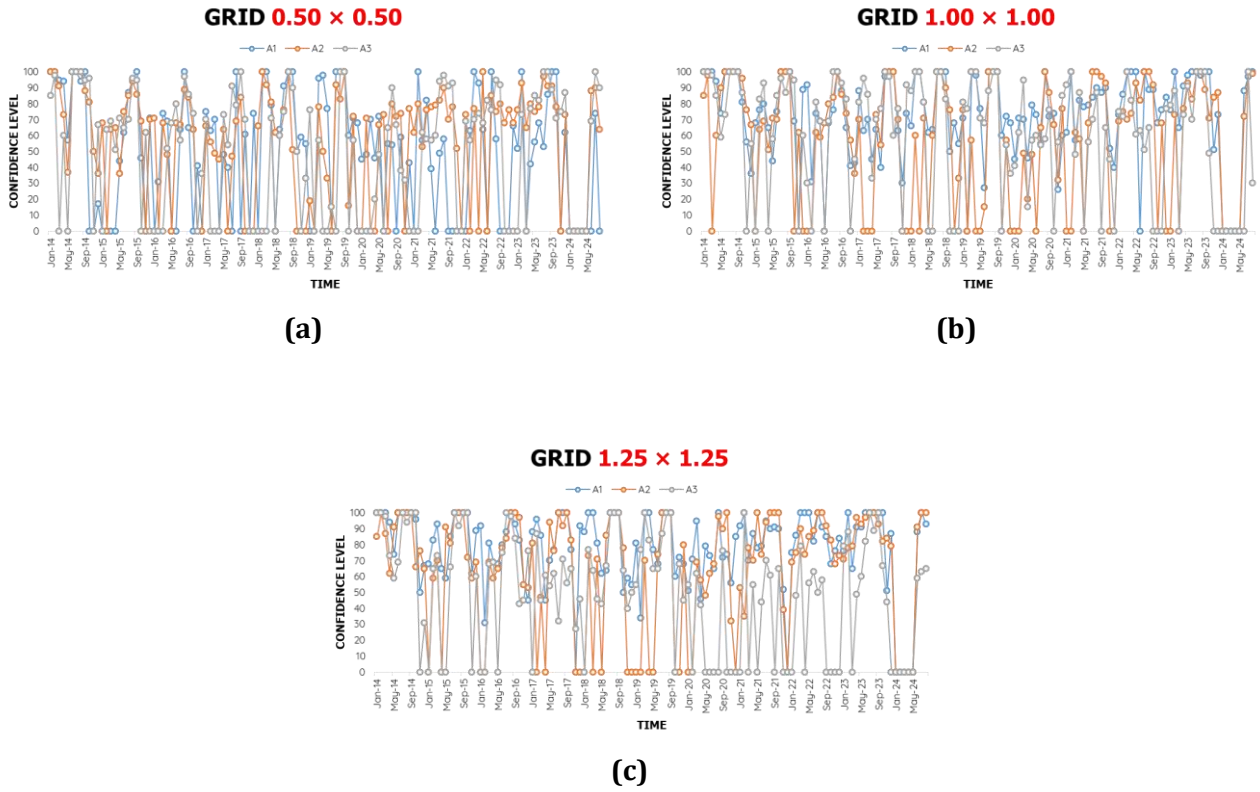
(a)

(b)

(c)

Figure 2. Data Plot of Hotspots of Forest Fires in West Kalimantan (a) 0.50×0.50 degrees (b) 1.00×1.00 degress (c) 1.25×1.25 degress

Table 2. Numerical Summary

Grid	Descriptive Statistics	Grid Cell										
		A1	A2	A3	A4	A5	A6	A7	A8	A9	A11	A12
0.50×0.50	Mean	48	55	48	6	56	48	2	35	48	16	29
	Median	55.5	68	60	0	66.5	56.5	0	0	56	0	0
	Maximum	100	100	100	95	100	100	87	100	100	100	100
1.00×1.00	Mean	73	55	59	65	16	54	-	-	-	-	-
	Median	76	68.5	70.5	70	0	70	-	-	-	-	-
	Maximum	100	100	100	100	100	100	-	-	-	-	-
1.25×1.25	Mean	78	64	50	58	-	-	-	-	-	-	-
	Median	85.5	76	59	69.5	-	-	-	-	-	-	-
	Maximum	100	100	100	100	-	-	-	-	-	-	-

The descriptive statistics of the hotspot data of forest fire cases in Kubu Raya and its surrounds are presented in Table 2, organized according to the various grid sizes, the red text is the highest value and the green text is the lowest value. The average results that were collected demonstrate variances in the confidence level of each grid unit regarding forest fire cases. An instance of a grid unit with a high average value may be observed at location A1 with a grid size of 1.25 × 1.25. This particular grid unit displays an average value of 78 and a median of 85.5. This score indicates that the forest fires at this location are highly intense and occur constantly. At this point, the maximum value exceeds 100, indicating that the fire in A1 has

reached the highest potential intensity. The average value recorded at position A7, which has a grid size of 0.50 × 0.50, is just 2, while the maximum value reaches 87. This is in contrast to the previously mentioned location. It is clear from this that fires in this area are extremely uncommon, and even when they do occur, the severity of the fires is significantly lower than in other areas. This gap demonstrates a significant disparity in the severity of forest fires in different Kubu Raya regions.
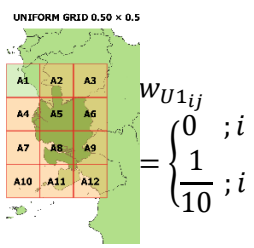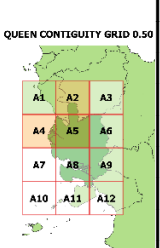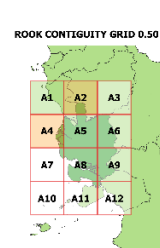
3. Stationarity Test

ADF and Box-Cox tests are tests that can be utilized to determine whether or not data is stationary. Based on the visualization of the data plot presented in Figure 2, one may conclude that the data is stationary with respect to both the mean and the variance. An ADF test was conducted to guarantee that the data was stationer the findings received from the test indicated that the p-value for all location grids was 0.01, which indicates that the p-value is less than 0.05. All of the location grids had stationary data.

4. Spatial Weight Matrix

Within the scope of this research, three distinct spatial weighting strategies are utilized: uniform, queen contiguity, and rook contiguity. Table 3 shows combining a grid with a spatial weight matrix, represented by the symbols W_{Uk}, W_{Qk}, and W_{Rk}, where $k = 1, 2, 3$.

Table 3. The Visualization of Each Grid and Spatial Weight Matrix

Uniform (W_{Uk})	Queen Contiguity (W_{Qk})	Rook Contiguity (W_{Rk})
	1. Grid: 0.50×0.50	

UNIFORM GRID 0.50 × 0.5

$$w_{U1_{ij}} = \begin{cases} 0 & ;i \\ \dfrac{1}{10} & ;i \end{cases}$$

QUEEN CONTIGUITY GRID 0.50

$$W_{Q1} = \begin{bmatrix}
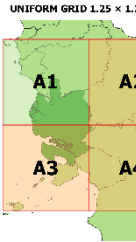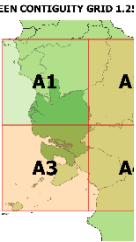0 & \frac{1}{3} & 0 & \frac{1}{3} & \frac{1}{3} & 0 & 0 & \cdots \\
\frac{1}{5} & 0 & \frac{1}{5} & \frac{1}{5} & \frac{1}{5} & \frac{1}{5} & 0 & \cdots \\
0 & \frac{1}{3} & 0 & 0 & \frac{1}{3} & \frac{1}{3} & 0 & \cdots \\
\frac{1}{5} & \frac{1}{5} & 0 & 0 & \frac{1}{5} & 0 & \frac{1}{5} & \cdots \\
\frac{1}{8} & \frac{1}{8} & \frac{1}{8} & \frac{1}{8} & 0 & \frac{1}{8} & \frac{1}{8} & \cdots \\
0 & \frac{1}{5} & \frac{1}{5} & 0 & \frac{1}{5} & 0 & 0 & \cdots \\
0 & 0 & 0 & \frac{1}{4} & \frac{1}{4} & 0 & 0 & \cdots \\
0 & 0 & 0 & \frac{1}{7} & \frac{1}{7} & \frac{1}{7} & \frac{1}{7} & \cdots \\
0 & 0 & 0 & 0 & \frac{1}{5} & \frac{1}{5} & 0 & \cdots \\
0 & 0 & 0 & 0 & 0 & 0 & \frac{1}{4} & \cdots \\
0 & 0 & 0 & 0 & 0 & 0 & 0 & \cdots
\end{bmatrix}$$

ROOK CONTIGUITY GRID 0.50

$$W_{R1} = \begin{bmatrix}
0 & \frac{1}{2} & 0 & \frac{1}{2} & 0 & 0 & 0 \\
\frac{1}{3} & 0 & \frac{1}{3} & 0 & \frac{1}{3} & 0 & 0 \\
0 & \frac{1}{2} & 0 & 0 & 0 & \frac{1}{2} & 0 \\
\frac{1}{3} & 0 & 0 & 0 & \frac{1}{3} & 0 & \frac{1}{3} \\
0 & \frac{1}{4} & 0 & \frac{1}{4} & 0 & \frac{1}{4} & 0 & \cdots \\
0 & 0 & \frac{1}{3} & 0 & \frac{1}{3} & 0 & 0 \\
0 & 0 & 0 & \frac{1}{2} & 0 & 0 & 0 & \cdots \\
0 & 0 & 0 & 0 & 0 & 0 & \frac{1}{3} \\
0 & 0 & 0 & 0 & 0 & \frac{1}{3} & 0 & \cdots \\
0 & 0 & 0 & 0 & 0 & 0 & 0
\end{bmatrix}$$

Uniform (W_{Uk})	Queen Contiguity (W_{Qk})	Rook Contiguity (W_{Rk})
	2. Grid: 1.00×1.00	
UNIFORM GRID 1.00 × 1. $w_{U2_{ij}} = \begin{cases} 0 & ; i \\ \frac{1}{5} & ; i = \end{cases}$	QUEEN CONTIGUITY GRID 1.00 $\begin{bmatrix} 0 & \frac{1}{3} & \frac{1}{3} & \frac{1}{3} & 0 & 0 \\ \frac{1}{3} & 0 & \frac{1}{3} & \frac{1}{3} & 0 & 0 \\ \frac{1}{5} & \frac{1}{5} & 0 & \frac{1}{5} & \frac{1}{5} & \frac{1}{5} \\ \frac{1}{5} & \frac{1}{5} & \frac{1}{5} & 0 & \frac{1}{5} & \frac{1}{5} \\ 0 & 0 & \frac{1}{3} & \frac{1}{3} & 0 & \frac{1}{3} \\ 0 & 0 & \frac{1}{3} & \frac{1}{3} & \frac{1}{3} & 0 \end{bmatrix}$	ROOK CONTIGUITY GRID 1.00 $\begin{bmatrix} 0 & \frac{1}{2} & \frac{1}{2} & 0 & 0 & 0 \\ \frac{1}{2} & 0 & 0 & \frac{1}{2} & 0 & 0 \\ \frac{1}{3} & 0 & 0 & \frac{1}{3} & \frac{1}{3} & 0 \\ 0 & \frac{1}{3} & \frac{1}{3} & 0 & 0 & \frac{1}{3} \\ 0 & 0 & \frac{1}{2} & 0 & 0 & \frac{1}{2} \\ 0 & 0 & 0 & \frac{1}{2} & \frac{1}{2} & 0 \end{bmatrix}$
	3. Grid: 1.25×1.25	
UNIFORM GRID 1.25 × 1. $w_{U3_{ij}} = \begin{cases} 0 & ; i \\ \frac{1}{3} & ; i = \end{cases}$	QUEEN CONTIGUITY GRID 1.25 $w_{Q3_{ij}} = \begin{cases} 0 & ; i = j \\ \frac{1}{3} & ; i \neq j \end{cases}$	ROOK CONTIGUITY GRID 1.25 $\begin{bmatrix} 0 & \frac{1}{2} & \frac{1}{2} & 0 \\ \frac{1}{2} & 0 & 0 & \frac{1}{2} \\ \frac{1}{2} & 0 & 0 & \frac{1}{2} \\ 0 & \frac{1}{2} & \frac{1}{2} & 0 \end{bmatrix}$

Every location is treated in the same manner and with the same weight when it comes to being deemed a neighbor of location A1. For location, the neighbors of location A1 in queen contiguity (second column in Table 3) are 0.50 × 0.50 (A2, A4, and A5), 1.00 × 1.00 (A2, A3, and A4), and 1.25 × 1.25 (A2, A3, and A4).

5. Parameter Estimation

The least squares method of parameter estimation reveals several substantial parameters. Using three different spatial weight matrices, the outcomes of the parameter estimation process were executed on the GSTAR (1;1) model for each grid in Table 4.

Table 4. Parameter Estimation, Diagnostic Test, and Accuracy of GSTAR (1;1) Model

Grid	Loc.	Parameter $\hat{\phi}_{10}$	Parameter $\hat{\phi}_{11}$	MAPE (%)	Diag. Test Norm.	Diag. Test Ind.	Grid	Loc.	Parameter $\hat{\phi}_{10}$	Parameter $\hat{\phi}_{11}$	MAPE (%)	Diag. Test Norm.	Diag. Test Ind.
						Uniform							
	A1	.178	.894	22.704	Yes	Yes		A1	.732	.258	9.443	Yes	No
	A2	.407	.678	19.018	Yes	Yes		A2	.376	.540	15.914	Yes	Yes
	A3	.418	.616	16.619	Yes	Yes	1.00 × 1.00	A3	.457	.452	15.991	Yes	No
	A4	.068	.159	5.925	No	Yes		A4	.447	.568	13.813	Yes	No
0.50 × 0.50	A5	.549	.428	17.130	Yes	Yes		A5	.315	.191	8.821	No	No
	A6	.487	.511	15.043	Yes	Yes		A6	.020	.946	16.154	Yes	Yes
	A7	.547	.028	1.310	No	No		Average			13.356		
	A8	.173	.702	17.705	Yes	Yes		A1	.896	.065	5.411	Yes	Yes
	A9	.416	.634	17.447	Yes	Yes	1.25 × 1.25	A2	.403	.549	12.545	Yes	Yes
	A11	.216	.364	8.721	No	No		A3	.274	.489	16.734	Yes	Yes
	A12	.194	.657	12.434	Yes	Yes		A4	.287	.618	12.468	No	Yes
	Average			14.005				Average			11.789		
						Queen Contiguity							
0	A1	.188	.793	21.831	Yes	Yes	1	A1	.578	.408	10.895	Yes	Yes

Grid	Loc.	$\hat{\phi}_{10}$	$\hat{\phi}_{11}$	MAPE (%)	Norm.	Ind.	Grid	Loc.	$\hat{\phi}_{10}$	$\hat{\phi}_{11}$	MAPE (%)	Norm.	Ind.
	A2	.318	.706	19.132	Yes	Yes		A2	.372	.465	15.015	Yes	Yes
	A3	.345	.502	16.312	Yes	Yes		A3	.457	.452	15.991	Yes	No
	A4	.075	.158	5.955	No	Yes		A4	.447	.568	13.813	Yes	No
	A5	.462	.559	17.151	Yes	Yes		A5	.312	.191	8.787	No	No
	A6	.353	.537	14.996	Yes	Yes		A6	.198	.815	16.563	Yes	Yes
	A7	.544	.033	1.308	No	No		Average			13.511		
	A8	.213	.738	17.661	Yes	Yes	1.25 × 1.25	A1	.896	.065	5.411	Yes	Yes
	A9	.536	.397	16.678	Yes	Yes		A2	.403	.549	12.545	Yes	Yes
	A11	.141	.477	8.709	No	No		A3	.274	.489	16.734	Yes	Yes
	A12	.260	.541	13.339	Yes	No		A4	.287	.618	12.468	No	Yes
	Average			13.916				Average			11.789		
Rook Contiguity													
	A1	.386	.641	20.615	Yes	Yes		A1	.680	.294	10.327	Yes	Yes
	A2	.335	.558	18.983	Yes	Yes	1.00 × 1.00	A2	.328	.490	15.173	Yes	Yes
	A3	.304	.553	17.217	Yes	Yes		A3	.403	.539	15.756	Yes	Yes
	A4	.085	.162	5.959	No	Yes		A4	.456	.505	14.493	Yes	Yes
0.50 × 0.50	A5	.504	.480	17.039	Yes	Yes		A5	.304	.198	8.710	No	No
	A6	.407	.453	13.601	Yes	Yes		A6	.259	.810	18.265	Yes	Yes
	A7	.540	.041	1.305	No	No		Average			13.787		
	A8	.433	.467	17.735	No	Yes		A1	.860	.115	5.540	Yes	Yes
	A9	.588	.318	16.367	Yes	Yes	1.25 × 1.25	A2	.353	.553	12.740	Yes	Yes
	A11	.179	.338	8.834	No	No		A3	.262	.490	16.437	Yes	Yes
	A12	.319	.502	13.210	Yes	Yes		A4	.381	.558	12.470	Yes	Yes
	Average			13.715				Average			11.797		

6. Diagnostic Test

The results of the diagnostic tests that were performed at each location are presented in Table 5. According to the white noise assumption, the combination of a grid with dimensions of 1.25 × 1.25 and a rook contiguity weight matrix has been successful. For the purpose of ensuring that the GSTAR (1;1) model functions exceptionally well for this grid, the residual models that are contained within the four location are regular and independent. A solid foundation is provided by this combination, which may be utilized for the research of forest fire patterns and the prediction of future events. As a result of the fact that it satisfies these criteria, the grid with dimensions of 1.25 × 1.25 and the rook contiguity weight matrix can be deemed the optimal combination.

7. Selection Of The Best Grid

The MAPE value for each grid and spatial weight matrix is within the range of 10% to 20%, which indicates a good level of accuracy. This information is provided in Table 4. Based on the results of this investigation, it is possible to draw the conclusion that the optimal grid size, as determined by the diagnostic test, is a grid with dimensions of 1.25 × 1.25 degrees and employing rook contiguity. As a result of the diagnostic test, the model with this combination has been able to pass the model feasibility test with a MAPE value of 11.789%. This demonstrates that the model is definitely capable of making more accurate predictions than alternative grid sizes and spatial weight matrices. For a grid with dimensions of 1.25 × 1.25 degrees, the GSTAR (1;1) model involves the utilization of the rook contiguity weight matrix. The equation can be expressed as follows:

$$Y_{T+m}^{(1)} = 0.860\ Y_{T+m-1}^{(1)} + 0.057\ Y_{T+m-1}^{(2)} + 0.057\ Y_{T+m-1}^{(3)} \tag{2}$$

$$Y_{T+m}^{(2)} = 0.277\ Y_{T+m-1}^{(1)} + 0.353\ Y_{T+m-1}^{(2)} + 0.277\ Y_{T+m-1}^{(4)} \tag{3}$$

$$Y_{T+m}^{(3)} = 0.245\ Y_{T+m-1}^{(1)} + 0.262\ Y_{T+m-1}^{(3)} + 0.245\ Y_{T+m-1}^{(4)} \tag{4}$$

$$Y_{T+m}^{(4)} = 0.279\ Y_{T+m-1}^{(2)} + 0.279\ Y_{T+m-1}^{(3)} + 0.381\ Y_{T+m-1}^{(4)} \tag{5}$$

The blue, red, green, and orange are respectively are for grid cell A1, A2, and A3.. The information presented by Equation (2), (3), (4), and (5) demonstrates that the maximum value of confidence level of forest fires on a particular grid cell is influenced by the maximum value of confidence level of forest fires on surrounding grid cells during the preceding period. Forest Fires cases on grid cell A1 is influenced by forest fires cases on grid cells A2, and, A3 in the preceding month, which had the same influence of 5.7%. This is an example of how forest fires might take location. Additionally, grid cell A1 was influenced by grid cell A1 itself in the preceding month by 86%. Table 5 presents the predictions made using the GSTAR (1;1) model.

Table 5. The Predictions Based on GSTAR (1;1) Model for The Best Combination Grid and Spatial Weight Matrix (%)

Period	A1	A2	A3	A4
September 2024	91	80	60	74
October 2024	86	74	56	67
November 2024	82	69	52	62
December 2024	77	64	49	57

D. CONCLUSION AND SUGGESTIONS

A grid with a dimension of 1.25 x 1.25 degrees and a rook contiguity weight matrix that has passed the model feasibility test with a MAPE value of 11.797%, which has a good level of accuracy, was deemed to be the optimal combination of grid and spatial weight matrix. This conclusion was reached based on the results and discussion discussed earlier. This demonstrates that in this particular investigation, a grid with a more significant size yields superior findings when compared to a grid with a smaller size at the same time. Therefore, this model can be utilized for the purpose of making forecasts for a number of different periods in the future, such that the prediction results for September, October, November, and December 2024 will show a declining trend in the number of forest fire instances.

REFERENCES

Arifa, N. M. (2022). *Kebakaran Hutan Kalimantan Barat Yang Mengakibatkan Terjadinya Kabut Asap Ekstrem Di Daerah Pontianak*. https://doi.org/10.31219/osf.io/4dqzy

Bill, R., Blankenbach, J., Breunig, M., Haunert, J.-H., Heipke, C., Herle, S., Maas, H.-G., Mayer, H., Meng, L., Rottensteiner, F., Schiewe, J., Sester, M., Sörgel, U., & Werner, M. (2022). Geospatial Information Research: State of the Art, Case Studies and Future Perspectives. *PFG – Journal of Photogrammetry, Remote Sensing and Geoinformation Science*, *90*(4), 349–389. https://doi.org/10.1007/s41064-022-00217-9

Dastour, H., Ahmed, M. R., & Hassan, Q. K. (2024). Analysis of forest fire patterns and their relationship with climate variables in Alberta's natural subregions. *Ecological Informatics*, *80*, 102531. https://doi.org/10.1016/j.ecoinf.2024.102531

Franch-Pardo, I., Napoletano, B. M., Rosete-Verges, F., & Billa, L. (2020). Spatial analysis and GIS in the study of COVID-19. A review. *Science of The Total Environment*, *739*, 140033.

https://doi.org/10.1016/j.scitotenv.2020.140033

Hestuningtias, F., & Kurniawan, M. H. S. (2023). The Implementation of the Generalized Space-Time Autoregressive (GSTAR) Model for Inflation Prediction. *Enthusiastic : International Journal of Applied Statistics and Data Science*, 176–188. https://doi.org/10.20885/enthusiastic.vol3.iss2.art5

Huda, N. M., Fran, F., Yundari, Y., Fikadila, L., & Safitri, F. (2023). Modified Weight Matrix Using Prim's Algorithm In Minimum Spanning Tree (MST) Aproach For GSTAR(1;1) Model. *BAREKENG: Jurnal Ilmu Matematika Dan Terapan*, *17*(1), 0263–0274. https://doi.org/10.30598/barekengvol17iss1pp0263-0274

Huda, N. M., & Imro'ah, N. (2023). Determination of the best weight matrix for the Generalized Space Time Autoregressive (GSTAR) model in the Covid-19 case on Java Island, Indonesia. *Spatial Statistics*, *54*, 100734. https://doi.org/10.1016/j.spasta.2023.100734

Huda, N. M., Mukhaiyar, U., & Imro'ah, N. (2022). An Iterative Procedure For Outlier Detection In GSTAR(1;1) Model. *BAREKENG: Jurnal Ilmu Matematika Dan Terapan*, *16*(3), 975–984. https://doi.org/10.30598/barekengvol16iss3pp975-984

Huda, N. M., Mukhaiyar, U., & Pasaribu, U. S. (2021). The approximation of GSTAR model for discrete cases through INAR model. *Journal of Physics: Conference Series*, *1722*(1), 012100. https://doi.org/10.1088/1742-6596/1722/1/012100

Ilmi, N., Aswi, A., & Aidid, M. K. (2023). Generalized Space Time Autoregressive Integrated Moving Average (GSTARIMA) dalam Peramalan Data Curah Hujan di Kota Makassar. *Inferensi*, *6*(1), 25. https://doi.org/10.12962/j27213862.v6i1.14347

Lam, C., & Souza, P. C. L. (2019). Estimation and Selection of Spatial Weight Matrix in a Spatial Lag Model. *Journal of Business & Economic Statistics*, *38*(3), 693–710. https://doi.org/10.1080/07350015.2019.1569526

Lu, X., Salehi, M., Haenggi, M., Hossain, E., & Jiang, H. (2021). Stochastic Geometry Analysis of Spatial-Temporal Performance in Wireless Networks: A Tutorial. *IEEE Communications Surveys & Tutorials*, *23*(4), 2753–2801. https://doi.org/10.1109/COMST.2021.3104581

Mukhaiyar, U., Huda, N. M., Novita Sari, R. K., & Pasaribu, U. S. (2019). Modeling Dengue Fever Cases by Using GSTAR(1;1) Model with Outlier Factor. *Journal of Physics: Conference Series*, *1366*(1), 012122. https://doi.org/10.1088/1742-6596/1366/1/012122

Pasaribu, U. S., Mukhaiyar, U., Huda, N. M., Sari, K. N., & Indratno, S. W. (2021). Modelling COVID-19 growth cases of provinces in java Island by modified spatial weight matrix GSTAR through railroad passenger's mobility. *Heliyon*, *7*(2), e06025. https://doi.org/10.1016/j.heliyon.2021.e06025

Rachman, A., Saharjo, B. H., & Putri, E. I. K. (2020). Forest and Land Fire Prevention Strategies in the Forest Management Unit Kubu Raya, South Ketapang, and North Ketapang in West Kalimantan Province. *Jurnal Ilmu Pertanian Indonesia*, *25*(2), 213–223. https://doi.org/10.18343/jipi.25.2.213

Ramsdale, J. D., Balme, M. R., Conway, S. J., Gallagher, C., van Gasselt, S. A., Hauber, E., Orgel, C., Séjourné, A., Skinner, J. A., Costard, F., Johnsson, A., Losiak, A., Reiss, D., Swirad, Z. M., Kereszturi, A., Smith, I. B., & Platz, T. (2017). Grid-based mapping: A method for rapidly determining the spatial distributions of small features over very large areas. *Planetary and Space Science*, *140*, 49–61. https://doi.org/10.1016/j.pss.2017.04.002

Ruchjana, B. N., Borovkova, S. A., & Lopuhaa, H. P. (2012). *Least squares estimation of Generalized Space Time AutoRegressive (GSTAR) model and its properties*. 61–64. https://doi.org/10.1063/1.4724118

Ryerson, M., Davidson, J., Wu, J. S., Feiglin, I., & Winston, F. (2022). Identifying community-level disparities in access to driver education and training: Toward a definition of driver training deserts. *Traffic Injury Prevention*, *23*(sup1). https://doi.org/10.1080/15389588.2022.2125305

Suryowati, K. S., Nahak, M., & Bekti, R. D. (2023). Penerapan Model Spasial Menggunakan Matriks Pembobot Queen Contiguity dan Euclidean Distance Terhadap Kasus Gizi Buruk Balita di Provinsi Nusa Tenggara Timur. *J Statistika: Jurnal Ilmiah Teori Dan Aplikasi Statistika*, *16*(1), 298–308. https://doi.org/10.36456/jstat.vol16.no1.a7871

Ware, C., Mayer, L., Johnson, P., Jakobsson, M., & Ferrini, V. (2020). A global geographic grid system for

visualizing bathymetry. *Geoscientific Instrumentation, Methods and Data Systems*, *9*(2), 375–384. https://doi.org/10.5194/gi-9-375-2020

Wu, Z., Wang, B., Li, M., Tian, Y., Quan, Y., & Liu, J. (2022). Simulation of forest fire spread based on artificial intelligence. *Ecological Indicators*, *136*, 108653. https://doi.org/10.1016/j.ecolind.2022.108653

Yundari, Pasaribu, U. S., Mukhaiyar, U., & Heriawan, M. N. (2018). Spatial Weight Determination of GSTAR(1;1) Model by Using Kernel Function. *Journal of Physics: Conference Series*, *1028*, 012223. https://doi.org/10.1088/1742-6596/1028/1/012223

Zhao, L., Sen Gupta, S., Khan, A., & Luo, R. (2021). Temporal Analysis of the Entire Ethereum Blockchain Network. *Proceedings of the Web Conference 2021*, 2258–2269. https://doi.org/10.1145/3442381.3449916

Zhu, P., Li, J., & Hou, Y. (2022). Applying a Population Flow–Based Spatial Weight Matrix in Spatial Econometric Models: Conceptual Framework and Application to COVID-19 Transmission Analysis. *Annals of the American Association of Geographers*, *112*(8), 2266–2286. https://doi.org/10.1080/24694452.2022.2060791